

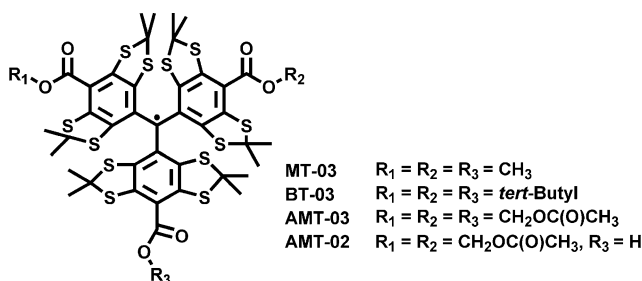
Synthesis and Characterization of Ester-Derivatized Tetrathiatriarylmethyl Radicals as Intracellular Oxygen Probes

Yangping Liu,[†] Frederick A. Villamena,^{*,†,‡} Jian Sun,[†] Yingkai Xu,[†]
Ilirian Dhimitruka,[†] and Jay L. Zweier^{*,†}

Center for Biomedical EPR Spectroscopy and Imaging, The Davis Heart and Lung Research Institute, the Division of Cardiovascular Medicine, Department of Internal Medicine, and Department of Pharmacology, College of Medicine, The Ohio State University, Columbus, Ohio 43210

jay.zweier@osumc.edu; frederick.villamena@osumc.edu

Received October 24, 2007



Electron paramagnetic resonance (EPR) spectroscopy using paramagnetic probes has been employed as an important tool for the accurate determination of oxygen (O₂) concentrations in biological systems. However, paramagnetic probes are still limited by their intracellular penetrability. Various esterified trityl derivatives were synthesized and characterized, and an X-ray structure of one of the triyl radicals was determined. The ester-derivatized trityls exhibited higher sensitivity to O₂ concentration compared to the trityl tricarboxylate CT-03. Cyclic voltammetry was also carried out to assess the susceptibility of the trityl radicals to oxidation and reduction. Among all of the ester-derivatized trityls studied, facile hydrolysis of the acetoxymethoxy esters to the respective carboxylate was observed using porcine liver esterase. This study demonstrates that cellular permeability of the trityl radicals can be achieved by varying the type and number of ester groups. Therefore, ester-derivatized trityl radicals show great potential as intracellular EPR oximetry probes and imaging agents.

1. Introduction

Molecular oxygen (O₂) as well as O₂-derived reactive species play an important role in normal cell function and are implicated in the pathogenesis of many diseases such as cancer, stroke, and ischemia-reperfusion injury.¹ Both hypoxic and hyperoxic conditions result in the generation of reactive oxygen species (ROS) which can cause cell injury or death.² There is, therefore,

a need for an accurate intracellular measurement of O₂ concentration to better understand cellular O₂ metabolism and the mechanisms of ROS-mediated cellular injury and disease.

Several techniques such as the Clark-type electrodes,³ fluorescence,⁴ ¹⁹F-nuclear magnetic resonance (NMR) spectroscopy,⁵ blood oxygen level-dependent imaging,⁶ and near-infrared

* To whom correspondence should be addressed. (J.L.Z.) Fax: 614-247-7845. (F.A.V.) Fax: 614-688-0999.

[†] Center for Biomedical EPR Spectroscopy and Imaging.

[‡] Department of Pharmacology.

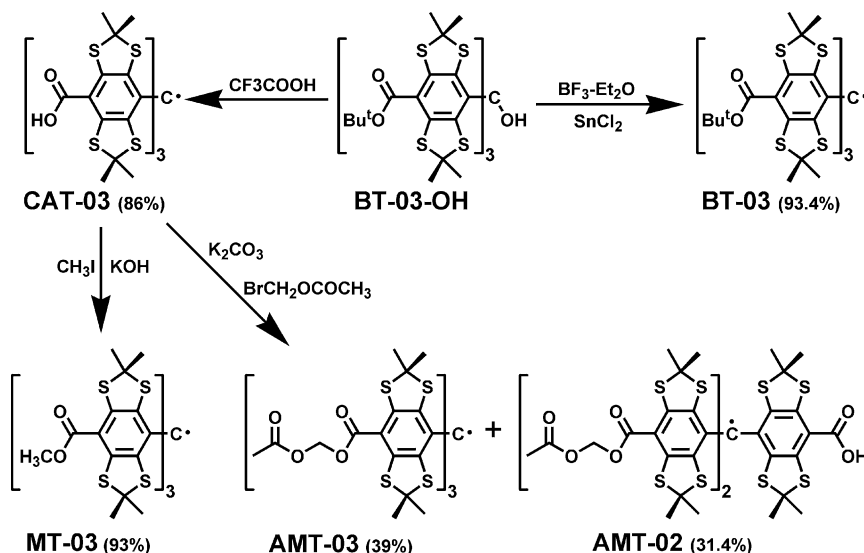
(1) (a) D'Angio, C. T.; Finkelstein, J. N. *Mol. Genet. Metab.* **2000**, *71*, 371. (b) Zweier, J. L.; Flaherty, J. T.; Weisfeldt, M. L. *Proc. Natl. Acad. Sci. U.S.A.* **1987**, *84*, 1404. (c) Clerch, L. B.; Massaro, D. J., Eds. *Oxygen, Gene Expression and Cellular Function*; Marcel Dekker: New York, 1997; Vol. 105. (d) Bilenko, M. V. *Ischemia and Reperfusion of Various Organs: Injury, Mechanisms, Methods of Prevention and Treatment*; Nova Science Pub., Inc.: Huntington, NY, 2001.

(2) (a) Finkel, T.; Holbrook, N. J. *Nature* **2000**, *408*, 239. (b) Halliwell, B.; Gutteridge, J. M. C. *Free Radicals in Biology and Medicine*; Oxford University Press: Oxford, 1999.

(3) (a) Pignitter, M.; Gorren, A. C. F.; Nedeianu, S.; Schmidt, K.; Mayer, B. *Free Radical Biol. Med.* **2006**, *41*, 455. (b) Kinugawa, S.; Zhang, J. H.; Messina, E.; Walsh, E.; Huang, H.; Kaminski, P. M.; Wolin, M. S.; Hintze, T. H. *Am. J. Physiol.* **2005**, *289*, H862. (c) Charbel, F. T.; Hoffman, W. E.; Misra, M.; Hannigan, K.; Ausman, J. I. *Surg. Neurol.* **1997**, *48*, 414.

(4) (a) O'Riordan, T. C.; Fitzgerald, K.; Ponomarev, G. V.; Mackrill, J.; Hynes, J.; Taylor, C.; Papkovsky, D. B. *Am. J. Physiol.* **2007**, *292*, R1613. (b) Shaw, A. D.; Li, Z.; Thomas, Z.; Stevens, C. W. *Circ. Care* **2002**, *6*, 76. (c) Braun, R. D.; Lanzen, J. L.; Snyder, S. A.; Dewhirst, M. W. *Am. J. Physiol.* **2001**, *280*, H2533.

SCHEME 1. Synthesis of Various Ester-Derivatized Trityl Radicals



imaging⁷ have been employed for the measurement of O_2 concentration in biological systems, but these methods are limited by sensitivity, invasiveness, and coverage of area being measured. Electron paramagnetic resonance (EPR) spectroscopy⁸ using O_2 -sensitive spin probes, however, has been a preferred technique due to its high specificity, sensitivity, and noninvasiveness.⁹

The Heisenberg exchange interaction of $^3\text{O}_2$ with paramagnetic centers results in EPR spectral line broadening. This line broadening phenomenon can be exploited to accurately measure the O_2 concentration in solution. Spin probes that have high stability and sensitivity to O_2 as well as narrow line width (ΔB_{pp}) in the presence of biological milieu are therefore desirable for in vitro and in vivo applications. Water-soluble paramagnetic probes such as nitroxides, trityl radicals, and India ink and particulate-based probes such as char and lithium phthalocyanine have been employed for $p\text{-O}_2$ or dissolved O_2 measurements in mouse tumor, brain, and heart using low-frequency EPR imaging.¹⁰ Among the commonly employed spin probes, ni-

troxides are the most popular but are limited by their instability due to their rapid bioreduction. Their presence of hyperfine splitting and moderately broad EPR line width limit the attainable resolution in spatial EPR imaging.¹¹ Recently, the synthesis of a series of tetrathiatritylmethyl (TAM) trityl radicals (Scheme 1) has been reported.¹² These paramagnetic species are preferred for in vivo EPR oximetry and imaging applications due to their high stability and narrow line width at physiological pH which provide high sensitivity and resolution for EPR imaging. Moreover, it has been shown that trityl radicals can be used as selective probes for superoxide radical,¹³ as a potential dual pH and oxygen probe,¹⁴ and as a reagent to assess the antioxidant activity of polyphenols.¹⁵ With linkage to specific ligands they are also ideally suitable to allow molecular imaging through EPR or Overhauser magnetic resonance imaging (MRI) techniques.

Recent efforts have been made on the preparation of anionic and hydrophilic trityl radicals such as CT-03, Ox063, and Ox031, and these compounds have found applications in EPRI and Overhauser MRI,¹⁶ but due to their charged nature, they

(5) (a) Laukemper-Ostendorf, S.; Scholz, A.; Burger, K.; Heussel, C. P.; Schmittner, M.; Weiler, N.; Markstaller, K.; Eberle, B.; Kauczor, H. U.; Quintel, M.; Thelen, M.; Schreiber, W. G. *Magn. Reson. Med.* **2002**, *47*, 82. (b) Zhao, D.; Constantinescu, A.; Jiang, L.; Hahn, E. W.; Mason, R. P. *Am. J. Clin. Oncol.* **2001**, *24*, 462. (c) Taylor, J.; Deutsch, C. *Biophys. J.* **1988**, *53*, 227.

(6) Kida, I.; Maciejewski, T. K.; Hyder, F. J. *Cereb. Blood Flow Metab.* **2004**, *24*, 1369.

(7) (a) O'Riordan, T. C.; Fitzgerald, K.; Ponomarev, G. V.; Mackrill, J.; Hynes, J.; Taylor, C.; Papkovsky, D. B. *Am. J. Physiol.* **2007**, *292*, R1613. (b) Xia, M.; Kodibagkar, V.; Liu, H.; Mason, R. P. *Phys. Med. Biol.* **2006**, *51*, 45. (c) Liu, H.; Gu, Y.; Kim, J. G.; Mason, R. P. *Method Enzymol.* **2004**, *386*, 349.

(8) Grucker, D. *Prog. Nucl. Magn. Reson. Spectrosc.* **2000**, *36*, 241.

(9) (a) He, G.; Shankar, R. A.; Chzhan, M.; Samouilov, A.; Kuppasamy, P.; Zweier, J. L. *Proc. Natl. Acad. Sci. U.S.A.* **1999**, *96*, 4586. (b) James, P. E.; Jackson, S. K.; Grinberg, O. Y.; Swartz, H. M. *Free Radical Biol. Med.* **1995**, *18*, 641. (c) Morse, P. D.; Swartz, H. M. *Magn. Reson. Med.* **1985**, *2*, 114. (d) Swartz, H. M.; Bacic, G.; Friedman, B.; Goda, F.; Grinberg, O. Y.; Hoopes, P. J.; Jiang, J. J.; Liu, K. J.; Nakashima, T.; O', Hara, J.; Walczak, T. *Adv. Exp. Med. Biol.* **1994**, *361*, 119. (e) Zweier, J. L.; Chzhan, M.; Ewert, U.; Schneider, G.; Kuppasamy, P. *J. Magn. Reson. B* **1994**, *105*, 52.

(10) (a) Williams, B. B.; Parasca, A.; Mailer, C.; Pelizzari, C. A.; Lewis, M. A.; River, J. N.; Karczmar, G. S.; Barth, E. D.; Halpern, H. J. *Magn. Reson. Med.* **2003**, *49*, 682. (b) Liu, S.; Timmins, G. S.; Shi, H.; Gasparovic, C. M.; Liu, K. J. *NMR Biomed.* **2004**, *17*, 5, 327. (c) Kuppasamy, P.; Zweier, J. L. *NMR Biomed.* **2004**, *17*, 5, 226.

(11) (a) Kocherginsky, N.; Swartz, H. M. *Nitroxide spin labels. Reactions in biology and chemistry*; CRC Press: Boca Raton, FL, 1995. (b) Swartz, H. M.; Timmins, G. S. In *Toxicology of the human environment: the critical role of free radicals*; Rhodes, C. J., Ed.; Taylor & Francis: London, 2000; p 91.

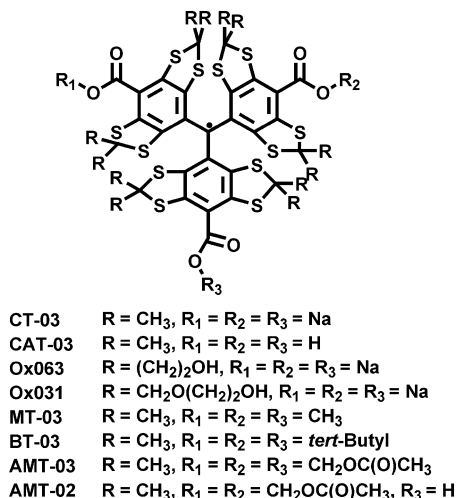
(12) (a) Joergensen, M.; Rise, F.; Andersson, S.; Almen, T.; Aabye, A.; Wistrand, L. G.; Wikstroem, H.; Golman, K.; Servin, R.; Michelsen, P. PCT Int. Appl. wo/9112024, 1991. (b) Andersson, S.; Radner, F.; Rydbeck, A.; Servin, R.; Wistrand, L. G. U. S. Patent 5530140, 1996. (c) Ardenkjaer-Larsen, J. H.; Leunbach, I. PCT Int. Appl. wo/9709633, 1997. (d) Andersson, S.; Radner, F.; Rydbeck, A.; Servin, R.; Wistrand, L.-G. U. S. Patent 5728370, 1998. (e) Thaning, M. PCT Int. Appl. wo/9839277, 1998. (f) Reddy, T. J.; Iwama, T.; Halpern, H. J.; Rawal, V. H. J. *Org. Chem.* **2002**, *67*, 4635. (g) Xia, S.; Villamena, F. A.; Hadad, C. M.; Kuppasamy, P.; Li, Y.; Zhu, H.; Zweier, J. L. *J. Org. Chem.* **2006**, *71*, 7268.

(13) Rizzi, C.; Samouilov, A.; Kumar Kutala, V.; Parinandi, N. L.; Zweier, J. L.; Kuppasamy, P. *Free Radical Biol. Med.* **2003**, *35*, 1608.

(14) Bobko, A. A.; Dhimitruka, I.; Zweier, J. L.; Khramtsov, V. V. *J. Am. Chem. Soc.* **2007**, *129*, 7240.

(15) Torres, J. L.; Carreras, A.; Jiménez, A.; Brillas, E.; Torrelles, X.; Rius, J.; Juliá, L. *J. Org. Chem.* **2007**, *72*, 3750.

(16) (a) Williams, B. B.; al Hallaq, H.; Chandramouli, G. V.; Barth, E. D.; Rivers, J. N.; Lewis, M.; Galtsev, V. E.; Karczmar, G. S.; Halpern, H. J. *Magn. Reson. Med.* **2002**, *47*, 634. (b) Ardenkjaer-Larsen, J. H.; Laursen, I.; Leunbach, I.; Ehnholm, G.; Wistrand, L.-G.; Petersson, J. S.; Golman, K. *J. Magn. Reson.* **1998**, *133*, 1.

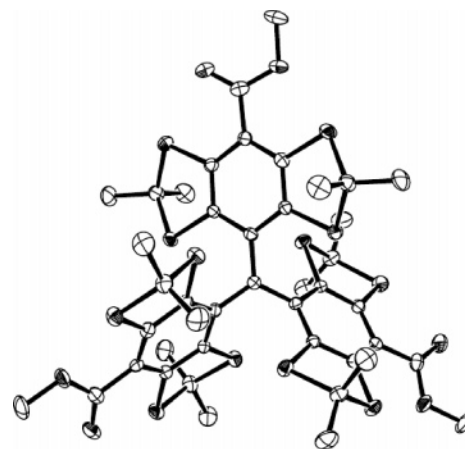
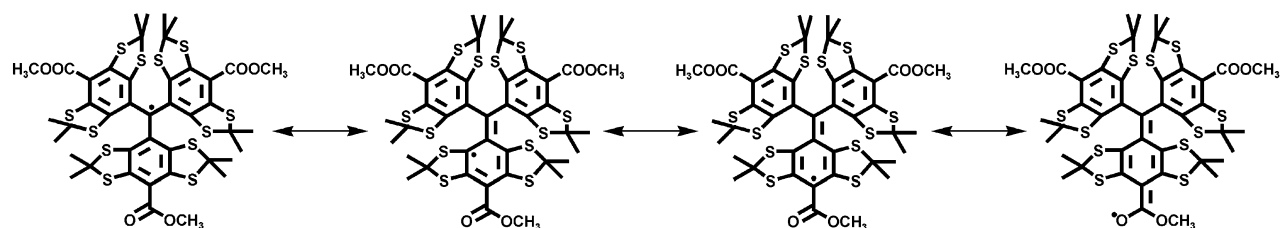
CHART 1. Molecular Structure of Various Trityl Radical Derivatives

do not enter cells and therefore are not useful as an intracellular O₂ probes (Chart 1). For example, CT-03, with pK_a ~4¹⁴ is anionic at physiological pH, and its intracellular penetrability is low even at high concentrations.

We now report the synthesis of several ester derivatives of CT-03 including AMT-03, AMT-02, MT-0, and BT-03 (see Chart 1), and their relative sensitivity to O₂ and redox properties were studied. The susceptibility to enzymatic hydrolysis of ester trityls to the corresponding acid is also reported.

2. Results and Discussion

2.1. Synthesis. The synthesis of TAM-type radicals in large scale for use in EPR imaging applications is limited due to the inefficient synthetic methodology used for their preparation.¹² Recently, we developed an improved method for the preparation of the trityl CAT-03 which allows synthesis of TAM-type compounds such as BT-03-OH in gram quantities.¹⁷ As shown in Scheme 1, reduction of BT-03-OH by BF₃–Et₂O and TFA afforded the trityl radical BT-03 (as a green solid) and CAT-03, respectively. Using the CAT-03 as a starting material, other esterified trityl radicals such as AMT-03 and AMT-02 were synthesized using bromomethyl acetate (or methyl iodide for MT-03) in basic medium. The use of KOH resulted in high yield (93%) in the case of MT-03 as green crystals which can be conveniently obtained by column chromatography followed by recrystallization. However, for the preparation of AMT-03 and AMT-02, the relatively weak base, K₂CO₃, was used instead of KOH in order to avoid possible hydrolysis of the ester, but this resulted to lower yields possibly due to the presence of starting material CAT-03 and monoester byproduct, hence making the separation more difficult. Detailed procedures on

SCHEME 2. Resonance Structure of MT-03**FIGURE 1. ORTEP view of the X-ray structure of MT-03.**

the ease and difficulty of synthesis of the various trityls are described in the Experimental Section.

2.2. X-ray Structure of MT-03. The X-ray crystallographic structure of MT-03 (see Figure 1) could provide useful insights into the electronic and chemical properties of the trityl derivatives. Structural analysis shows experimental bond angles between the aromatic-carbon and the central-carbon atoms of 119.994(8)°. However, the bond distance of 1.449(3) Å between the central-carbon and aromatic-carbon atoms is intermediate between the reported C_{sp3}–aryl bond distance in diamagnetic compounds and that of the double bond distance in C=C–C=C systems of 1.506(3) Å¹⁸ and 1.358(3) Å,¹⁹ respectively, indicating the existence of several resonance contributions as shown in Scheme 2. To further support these resonance forms proposed in Scheme 2, spin density analyses at the B3LYP/6-311+G**//B3LYP/6-31+G* level were carried out and showed spin delocalization of 0.075–0.084 e on the ortho carbons, 0.066–0.069 e on the para carbons, and 0.014–0.015 e on the carbonyl oxygens (see the Supporting Information for a complete list of the spin densities for MT-03) indicating a partial sp² hybridization on the central-carbon. This hybridization supports the formation of a P₄ plane along the central-carbon and the aromatic-carbons making MT-03 bear the molecular structure of a C₃ symmetry in which the three phenyl rings are almost perpendicular to each other with an angle of 75.6(1)°. The steric repulsion resulting from the bulky substituent of the aromatic ring also forces the ester groups to slightly deviate from the plane of the phenyl ring with an angle of 17.0(3)°. Furthermore, the two five-membered thio-groups on each phenyl ring also provide significant steric protection of the central carbon atom which may be responsible for the high stability of the trityl radicals in chemical and biological systems.

2.3. EPR Characteristics. 2.3.1. Hyperfine Structures and Linewidths. Under anaerobic conditions, the newly synthesized TAM-type radicals exhibit a single sharp EPR spectrum with

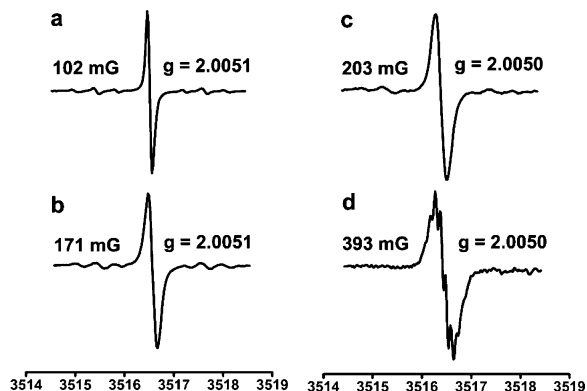


FIGURE 2. X-band EPR spectra, linewidths (ΔB_{pp}), and g -tensors of (a) BT-03; (b) AMT-03; (c) AMT-02; and (d) MT-03 in DMSO under anaerobic conditions.

linewidths of $\Delta B_{pp} = 102\text{--}203$ mG as shown in Figure 2, except in the case of MT-03 ($\Delta B_{pp} = 393$ mG) where small hyperfine structure (hfs) was observed due to interaction between the unpaired electron and the protons of the three methoxycarbonyl groups and as a result of extensive π conjugation along the central carbon, aryl, and the ester group. The differences in ΔB_{pp} between BT-03, AMT-03, and AMT-02 may be due to the number of alkoxy protons and their relative distance to the O-esters where the unpaired electron also resides. The proton hfs of 106 mG observed in MT-03 is considerably smaller than that observed in triphenylmethyl radical ($a_H = 2.745$ G)²⁰ and trityl radicals with an unsubstituted aromatic group ($a_H = 2.3$ G).^{12g} To further confirm these a_H assignments, the spin density distribution in various trityl radicals was theoretically determined using density functional theory (DFT),^{21,22} and results show that the methoxy-H's in MT-03 have smaller spin density distribution (0.00015 e) compared to the aromatic protons in triphenylmethyl radical (0.00365 e) and the partially substituted tetrathiatriarylmethyl radicals (0.00281 e).^{12g} In general, the differences in anaerobic ΔB_{pp} among the trityl radicals are most likely due to the resolved or unresolved hfs.²³ Spin relaxation, however, may have a minor effect on the differences in the observed ΔB_{pp} since there are only minor variations in the molecular structure of the ester-derivatized trityl radicals, assuming that all of the trityls have the same solubility and mode of solvation in DMSO.

2.3.2. Sensitivity of Line Width Broadening to O₂ Concentration. Line broadening phenomenon via formation of collision complexes has been observed for nitroxides in the presence of O₂.²⁴ The effect of spin exchange between the esterified trityl and O₂ on the EPR spectral line broadening in DMSO is shown in Figure 3. The ΔB_{pp} of each of the trityl radicals increases linearly as a function of O₂ concentration and

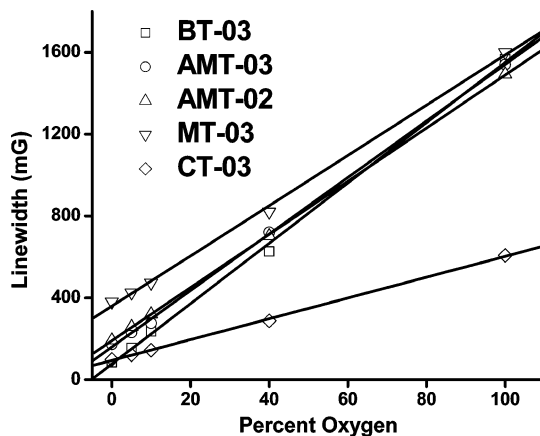


FIGURE 3. Plots of linewidths (ΔB_{pp}) of (□) BT-03, (○) AMT-03, (△) AMT-02, (▽) MT-03, and (◇) CT-03 as a function of O₂ concentration in DMSO (CT-03 was performed in PBS buffer).

reaches similar maxima at 100% O₂. For comparison, the EPR spectral line broadening of the water soluble trityl, CT-03, as a function of O₂ concentration was also determined and compared with the ester derivatives.

Varying sensitivity to O₂ concentration was observed for some of the trityls as shown by the different slopes in Figure 3. The order of decreasing slope (and therefore sensitivity) is as follows (in mG/%O₂ ± SD): BT-03 (14.74 ± 0.31) > AMT-03 (13.81 ± 0.19) > AMT-02 (12.99 ± 0.06) > MT-03 (12.28 ± 0.28) ≫ CT-03 (5.09 ± 0.08 in H₂O). In general, the four ester-derivatized trityls are more sensitive to O₂ concentration than CT-03 due to higher solubility of ester-derivatized trityls and O₂ in DMSO resulting to a more efficient collision between them in solution. Furthermore, the highest slope observed for BT-03 could be due to the small unresolved hfs making this compound more sensitive to EPR spectral line broadening, while the low sensitivity of MT-03 to O₂ could be due to its already broader peak due to resolved hfs. For CT-03, the lower solubility of O₂ in water than in DMSO as well as electrostatic repulsion of the charge species with O₂ can result in the lower O₂ sensitivity. These results suggest that the resolved and unresolved hfs as well as compound and O₂ solubility can play an important role in the anaerobic line width and O₂-dependent line broadening response of the trityl radicals.

2.4. Cyclic Voltammetry Studies. Cyclic voltammetry (CV) was used to investigate the redox behavior of the ester-derivatized trityl radicals in dichloromethane (DCM). Cyclic voltammograms of the trityl radicals gave one-electron reduction and oxidation waves, as shown in Figure 4. One-electron oxidation of the trityl radicals MT-03, BT-03, and AMT-03 to the corresponding trityl cations was reversible, but in the case of AMT-02, the first oxidation was irreversible and with the second oxidation gave a reversible couple that corresponds to the production of the trityl cation. At the cathodic region, different electrochemical behavior was observed upon reduction of the trityls. While the one-electron reduction of AMT-03 and MT-03 were found to be reversible, the reduction of BT-03 was irreversible. For AMT-02, the first reduction was irreversible

(17) Dhimitruka, I.; Velayutham, M.; Bobko, A. A.; Khramtsov, V. V.; Villamena, F. A.; Hadad, C. M.; Zweier, J. L. *Bioorg. Med. Chem. Lett.* **2007**, 6801.

(18) Luo, Y. P.; Zhou, H. B. *Acta Crystallogr. E* **2006**, 62, O5369.

(19) Wu, A. S.; Li, X. G.; He, L. L.; Wang, S. R. *Acta Crystallogr. E* **2005**, 61, O3699.

(20) Trapp, C.; Kulkarni, S. V. *J. Phys. Chem.* **1984**, 88, 2703.

(21) Labanowski, J. W.; Andzelm, J. *Density Functional Methods in Chemistry*; Springer: New York, 1991.

(22) Parr, R. G.; Yang, W. *Density Functional Theory in Atoms and Molecules*; Oxford University Press: New York, 1989.

(23) (a) Bowman, M. K.; Mailer, C.; Halpern, H. J. *J. Magn. Reson.* **2005**, 172, 254. (b) Yong, L.; Harbridge, J.; Quine, R. W.; Rinard, G. A.; Eaton, S. S.; Eaton, G. R.; Mailer, C.; Barth, E.; Halpern, H. J. *J. Magn. Reson.* **2001**, 152, 156.

(24) (a) Morrisett, J. D. In *Spin Labeling. Theory and Applications*; Berliner, L. J., Ed.; Academic Press: New York, 1976. (b) Hyde, J. S.; Subczynski, W. K. In *Biological Magnetic Resonance*; Berliner, L. J., Reuben, J., Eds.; Plenum Press: New York, 1978; Vol. 8, p 339. (c) Moscatelli, A.; Ottaviani, M. F.; Adam, W.; Buchachenko, A.; Jockusch, S.; Turro, N. J. *Helv. Chim. Acta* **2006**, 89, 2441.

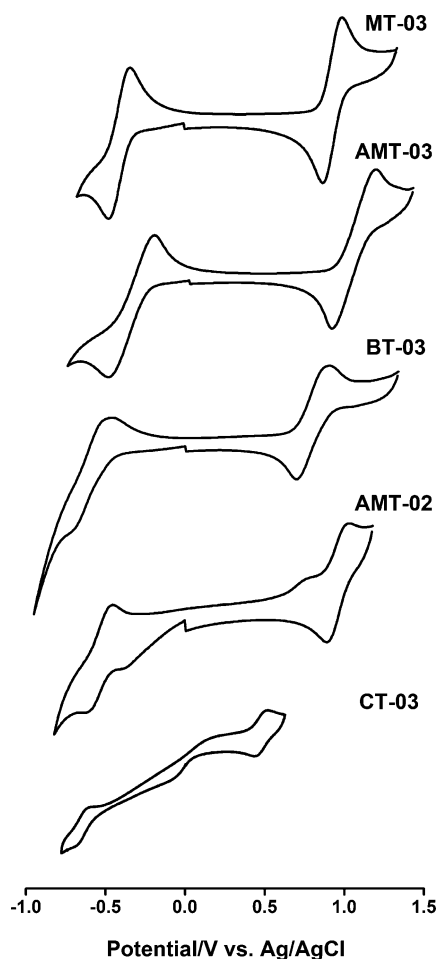


FIGURE 4. Cyclic voltammogram of 1 mM ester-derivatized trityl radicals in dichloromethane containing 0.1 M tetrabutylammonium perchlorate and 1 mM CT-03 in water containing 0.15 M KCl. Scan rates = 50 mV/s except for CT-03 in which a scan rate of 10 mV/s was used.

but the second reduction peak was reversible. As a comparison, we also investigated the electrochemical behavior of the hydrophilic trityl radical CT-03. As shown in Figure 4, the one-electron reduction and oxidation of CT-03 show reversible couple with peak separations equal to 69 and 66 mV, respectively.

The observed peak separations (ΔE_p) for the ester-derivatized trityls were in the range of 118–224 mV (Table 1), larger than Nernstian one-electron wave (ΔE_p) of 59 mV. However, TEMPO and ferrocene (Fc), whose oxidations are known to show Nernstian behavior, gave large ΔE_p with a value of 196 and 136 mV, respectively, under the same experimental conditions (Table 1). The large ΔE_p 's are most likely due to the nonpolar nature of DCM. To confirm the solvent polarity effect on the ΔE_p 's, cyclic voltammetry was carried out using AMT-03 in a more polar solvent such as MeCN and gave a considerably smaller ΔE_p value of 88 mV for both reduction and oxidation peaks compared to 229 mV (oxidation) and 209 mV (reduction) in DCM. Additionally, the cathodic and anodic peak current ratios i_{pc}/i_{pa} for the oxidation and reduction waves of MT-03 and AMT-03, and second oxidation and reduction waves of AMT-02 were approximately unity at the studied scan rates, while the anodic and reverse cathodic peak currents were proportional to $\nu^{1/2}$.

TABLE 1. Redox Potentials ($E_{1/2}$) of Trityl Radicals versus Fc^+/Fc Determined by Cyclic Voltammetry^a

trityl radical	solvent	$E_{1/2}$ (red)/V (ΔE_p /mV) ^b	$E_{1/2}$ (ox)/V (ΔE_p /mV) ^b
MT-03	CH ₂ Cl ₂	-0.912 (133)	0.414 (118)
AMT-03	CH ₂ Cl ₂	-0.872 (224)	0.492 (209)
BT-03	CH ₂ Cl ₂	-1.083 (219)	0.292 (195)
AMT-02	CH ₂ Cl ₂	-0.878, ^c -1.033 (128) ^d	0.232, ^e 0.421 (122) ^f
CT-03	CH ₂ Cl ₂ ^g	-0.891	0.194
CT-03	water	-0.626 (69)	0.458 (66)
TEMPO	water	-0.739 ^c	0.525 (68)
TEMPO	CH ₂ Cl ₂		0.764 (196)
ferrocene	CH ₂ Cl ₂		0.503 (136)

^a The redox potentials of the ester trityls were referenced internally using ferrocene. ^b $\Delta E_p = |E_p^a - E_p^c|$. ^c Cathodic peak only. ^d Second reduction. ^e Anodic peak only. ^f Second oxidation. ^g Value obtained using the potential difference of $E_{DCM} - E_{water} = 0.239$ V for TEMPO and the oxidation potential of ferrocene (0.503 V) in CH₂Cl₂.

As shown in Table 1, substituent effect on the redox potentials was observed. The trend in half-wave potentials ($E_{1/2}$ (red)) vs Fc^+/Fc for the reduction of the triester-substituted trityls were BT-03 (-1.083 V) > MT-03 (-0.912 V) > AMT-03 (-0.872 V) and shift cathodically in the presence of stronger electron-withdrawing group. Substitution of *tert*-butoxycarbonyl group in BT-03 with more electron withdrawing acetoxymethoxycarbonyl group in AMT-03 can lead to lowering the LUMO energy hence stabilizing the trityl anion form. The electron-withdrawing property of acetoxyl moiety on alkyl groups has been reported previously.²⁵ The order of increasing half-wave oxidation potentials ($E_{1/2}$) vs Fc^+/Fc was as follows: BT-03 (0.292 V) < MT-03 (0.414 V) < AMT-03 (0.492 V) and shift anodically with increasing electron-withdrawing effect of the substituent due probably to the destabilization of the cation formed. Trityl, AMT-02, gave the least negative reduction and positive oxidation peaks at -0.878 and 0.232 V vs Fc^+/Fc , respectively, relative to AMT-03. This difference is due to the presence of carboxylic acid moiety in AMT-02 which is more electron withdrawing than the ester group.

The acid trityl, CT-03, shows a relatively negative $E_{1/2}$ (red) (-0.626 V) and small $E_{1/2}$ (ox) (0.458 V) in 0.15 M KCl solution. Calibration of CT-03 redox potentials in DCM using TEMPO as standard gave $E_{1/2}$ (red) = -0.387 V and $E_{1/2}$ (ox) = 0.697 V which is based on the value of Fc^+/Fc (0.503 V) in DCM and further referenced to $E_{1/2}$ (red) = -0.891 V vs Fc^+/Fc and $E_{1/2}$ (ox) = 0.194 V vs Fc^+/Fc . Therefore, the order of increasing thermodynamic tendency for reduction of various trityls in DCM is as follows: BT-03 < MT-03 < CT-03 < AMT-03 < AMT-02, while the order of increasing tendency to be oxidized is AMT-03 < MT-03 < BT-03 < AMT-02 ~ CT-03. This study demonstrates that esterification of the trityl radical can have significant effect on their redox activity and provides important insight toward design of more stable trityls. However, these redox potentials may not explain their redox activity in physiological conditions since redox potential is a thermodynamic entity. Kinetic factors should also be considered in assessing their biostability in the presence of bioreductants

(25) (a) Cha, J. S.; Nam, H. T.; Park, S. J.; Kwon, S. Y.; Kwon, O. O. *Bull. Korean Chem. Soc.* **2006**, *27*, 667. (b) Jin, D. Z.; Kwon, S. H.; Moon, H. R.; Gunaga, P.; Kim, H. O.; Kim, D. K.; Chun, M. W.; Jeong, L. S. *Bioorg. Med. Chem.* **2004**, *12*, 1101. (c) Ouedraogo, A.; Lessard, J. *Can. J. Chem.* **1991**, *69*, 474. (d) Ouedraogo, A.; Viet, M. T. P.; Saunders, J. K.; Lessard, J. *Can. J. Chem.* **1987**, *65*, 1761.

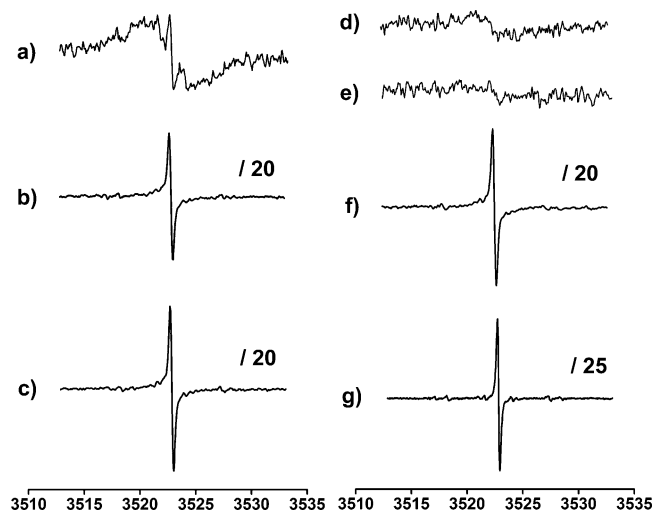


FIGURE 5. EPR spectra upon hydrolysis of the ester-derivatized trityl radicals ($10 \mu\text{M}$) with PLE (50 U/mL) at 37°C in PBS buffer containing 5% DMSO at various incubation times: (a) AMT-02, 0 min; (b) AMT-02, 15 min; (c) AMT-02, 45 min; (d) MT-03, 60 min; (e) BT-03, 60 min; (f) AMT-03, 60 min (using 10% DMSO); (g) CT-03 ($10 \mu\text{M}$). The EPR intensities of parts b, c, and f were reduced by 20-fold and that of g was reduced by 25-fold.

since microenvironments such as pH, temperature, or steric effect can have significant effect.

2.5. Enzymatic Hydrolysis Studies. Cytosolic esterases can hydrolyze esters into acids or carboxylates. This strategy has been widely employed for intracellular labeling and drug delivery.²⁶ To test if the synthesized ester-derivatized trityls can be enzymatically hydrolyzed to CT-03, solutions of the trityl radicals in 5%–95% or 10%–90% DMSO–PBS (v/v) (pH 7.4) were each incubated with porcine liver esterase (PLE).

The EPR spectrum of AMT-02 solution (Figure 5a) prior to incubation with PLE shows two components which consists of sharp and broad signals with ΔB_{pp} of $\sim 350 \text{ mG}$ and 4.76 G , respectively. The sharp and broad signals could be due to a mixture of dissolved and undissolved or aggregated form of AMT-02. After incubation, only the sharp signal with $\Delta B_{pp} = 230 \text{ mG}$ can be observed (see parts b and c of Figure 5). The ΔB_{pp} observed for AMT-02 after incubation is slightly broader compared to CT-03 (i.e., $\Delta B_{pp} = 190 \text{ mG}$) and is narrower compared to before incubation (i.e., $\Delta B_{pp} = 350 \text{ mG}$). To confirm if the newly observed ΔB_{pp} after incubation is due to the binding of trityl with PLE, a solution of CT-03 ($10 \mu\text{M}$) was added to PLE solution and gave an EPR signal with ΔB_{pp} of 227 mG . The line width broadening could be due to shorter T_2 relaxivity of the trityl upon binding to PLE, and similar binding of trityl to protein was also previously observed.^{14b} This study further confirms that AMT-02 can be hydrolyzed to CT-03 by PLE.

The production of CT-03 was also dependent on the incubation time as shown by the increase in EPR signal intensity (Figure 6) and begins to plateau after 60 min of incubation, indicating that the hydrolysis of AMT-02 is nearly complete at this point. In contrast, there are no significant changes in the

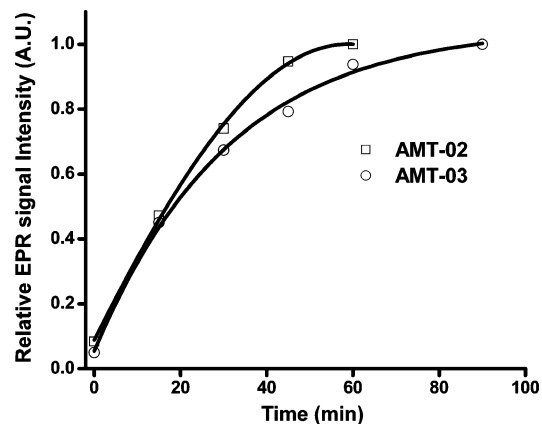


FIGURE 6. Relative EPR signal intensity as a function of time of incubation. Incubation was performed in the presence of PLE (50 U/mL) at 37°C in PBS buffer containing 5% DMSO for AMT-02 ($10 \mu\text{M}$) or 10% DMSO for AMT-03 ($10 \mu\text{M}$).

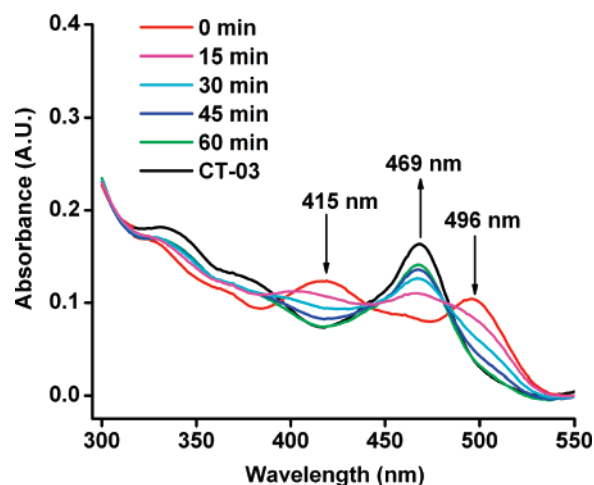


FIGURE 7. UV–vis spectra of $10 \mu\text{M}$ AMT-02 in PBS with 5% DMSO incubated over a period of 0–60 min with PLE (50 U/mL) at 37°C .

EPR signal intensity and/or line width of AMT-03, MT-03, and BT-03 even after 60 min of incubation with PLE at 5% DMSO due probably to their high hydrophobicity in which only broad and weak signals were observed in solution (see parts d and e of Figures 5) even after increasing the PLE concentration and incubation time. Also, the fact that BT-03 and MT-03 were not hydrolyzed by the PLE could be attributed to the steric hindrance of the respective alkoxy moiety.

Due to the poor solubility of AMT-03, MT-03, and BT-03 in water, the enzymatic hydrolysis of esters at higher DMSO concentration (10% DMSO in PBS) was investigated. Hydrolysis of AMT-03 to CT-03 was observed, however, a longer incubation time of $\sim 90 \text{ min}$ was required to complete the hydrolysis (Figure 6). No observable hydrolysis was observed for BT-03 and MT-03. It can, therefore, be inferred that trityl radicals containing the acetoxymethoxycarbonyl group are more prone to hydrolysis than those containing the methoxycarbonyl and *tert*-butoxycarbonyl groups.

In order to further confirm that the hydrolysis of AMT-02 would result in the production of CT-03, we performed spectrophotometric measurement to examine the hydrolysis of AMT-02 by PLE. Figure 7 illustrates the changes in UV spectrum of AMT-02 as a function of time in the presence of

(26) (a) Velazquez, C.; Rao, P. N. P.; Knaus, E. E. *J. Med. Chem.* **2005**, *48*, 4061. (b) He, X.; Lu, W.; Jiang, X.; Cai, J.; Zhang, X.; Ding, J. *Bioorg. Med. Chem.* **2004**, *12*, 4003. (c) Labaree, D. C.; Zhang, J. X.; Harris, H. A.; O'Connor, C.; Reynolds, T. Y.; Hochberg, R. B. *J. Med. Chem.* **2003**, *46*, 1886; (d) Ostacolo, C.; Marra, F.; Laneri, S.; Sacchi, A.; Nicoli, S.; Padula, C.; Santi, P. *J. Control. Release* **2004**, *99*, 403.

PLE. Before incubation, AMT-02 has two maximum absorbances at 415 and 496 nm whose intensities decrease as a function of time of incubation, while a new peak at 469 nm characteristic of CT-03 appears. After 60 min of incubation, the 415 and 496 nm peaks completely disappeared and the 469 nm peak reached its maximum, indicating that the hydrolysis of AMT-02 is almost complete at this point. The hydrolysis of AMT-03 in 10% DMSO–PBS by PLE to form CT-03 was also observed. Moreover, EPR and UV–vis spectroscopy showed that hydrolysis of 10 μ M AMT-02 to CT-03 was chemically achieved using 2.5 mM KOH, but complete hydrolysis required a longer reaction time of about 90 min. This UV–vis spectroscopic study further confirms the conversion of AMT-02 and AMT-03 to CT-03 by PLE and is consistent with the EPR results.

3. Conclusions

Various ester-substituted trityls have been synthesized and characterized, and their EPR spectral properties were investigated. The sensitivity of the trityl EPR line width to O₂ is governed by facile spin–spin interaction and solubility in DMSO with the highest sensitivity observed for BT-03. Redox properties of the trityls were also influenced by the nature of the ester-substituents and provide important insights toward the design of trityls with high stability toward reduction and oxidation. Esterase-mediated hydrolysis of trityls bearing acetoxymethoxy moiety (e.g., AMT-02 and AMT-03) was more facile compared to methyl and *tert*-butyl ester-derivatized trityls (such as BT-03 and MT-03). This study demonstrates the feasibility of some ester-derivatives to be enzymatically hydrolyzed and establishes their potential use as intracellular O₂ probes. Intracellular permeability and hydrolysis studies are now ongoing in our laboratory.

4. Experimental Section

General Procedures. All other reagents were obtained commercially and used without further purification. Reactions were carried out under dry nitrogen atmosphere using standard Schlenk techniques unless otherwise indicated. Tris(8-*tert*-butoxycarboxyl-2,2,6,6-tetramethylbenzo[1,2-*d*;4,5-*d'*]bis[1,3]dithiol-4-yl)methanol (BT-03-OH) was synthesized using tetra-*tert*-butylthiobenzene as a starting material according to the previous procedure.¹⁷ The trityl radical purity was determined using TEMPO as standard. In a typical experiment, purified trityl was weighed and dissolved in DMSO. The EPR spectrum was obtained and peak area was determined using double integration. The concentration of the trityl radical was then determined using a standard curve of known concentration of TEMPO versus peak area (see Figure S12 in the Supporting Information). Each experiment was done in triplicate. The paramagnetic purity for all the trityl radicals was determined to be >95%.

Tris(8-carboxy-2,2,6,6-tetramethylbenzo[1,2-*d*;4,5-*d'*]bis[1,3]dithiol-4-yl)methyl (CAT-03). The trityl alcohol BT-03 was synthesized according to the procedure previously described.¹⁷ To the solid BT-03-OH (1.0 g, 0.92 mmol) was added 10 mL of trifluoroacetic acid. The solution was exposed to air and stirred for 24 h at room temperature. The reaction mixture was then dried using high vacuum and treated with aqueous NaOH solution (4 equiv) to remove the insoluble impurities. The resulting green solution was then acidified using 1 M HCl until the brown solid precipitate was formed and then filtered. This procedure was repeated twice to yield the brown solid CAT-03 (0.79 g, 0.79 mmol, 86%): IR (cm⁻¹, neat) 3514 (broad), 2967, 2922, 1688, 1490, 1453,

1366, 1231, 1149, 867, 726; UV–vis (λ_{max} , nm, MeOH) 268 ($\epsilon = 38.1 \text{ mM}^{-1} \text{ cm}^{-1}$), 469 ($16.7 \text{ mM}^{-1} \text{ cm}^{-1}$).

Tris(8-*tert*-butoxycarboxyl-2,2,6,6-tetramethylbenzo[1,2-*d*;4,5-*d'*]bis[1,3]dithiol-4-yl)methyl (BT-03). BF₃·Et₂O (78 μ L, 0.62 mmol) was added dropwise to a stirred solution of BT-03-OH in CH₂Cl₂ (92 mg, 0.078 mmol) at room temperature. The reaction mixture was stirred for 1 h and then treated with a solution of SnCl₂ (25 mg, 0.133 mmol) in THF. After 10 min, saturated aqueous solution of KH₂PO₄ was added. The organic layer was separated, dried over Na₂SO₄, and concentrated in vacuo. The crude product was separated by chromatography using the eluent (20:1 CH₂Cl₂/MeOH) to afford the green solid BT-03 (85 mg, 93.4%): IR (cm⁻¹, neat) 2976, 2924, 1695, 1486, 1454, 1366, 1312, 1280, 1238, 1163, 1135, 1111, 1033, 847, 687; UV–vis (λ_{max} , nm, in CH₂Cl₂) 268 ($\epsilon = 47.3 \text{ mM}^{-1} \text{ cm}^{-1}$), 400 ($\epsilon = 16.1 \text{ mM}^{-1} \text{ cm}^{-1}$), 487 ($\epsilon = 18.7 \text{ mM}^{-1} \text{ cm}^{-1}$); MS (ESI, [M+Na]⁺, *m/z*) 1190.1150 (measured), 1190.1171 (calcd).

Tris(8-methoxycarbonyl-2,2,6,6-tetramethylbenzo[1,2-*d*;4,5-*d'*]bis[1,3]dithiol-4-yl)methyl (MT-03). Solid KOH (108 mg, 1.93 mmol) was added to a solution of CAT-03 (202 mg, 0.21 mmol) in 10 mL of DMSO. The reaction mixture was stirred for 0.5 h, and CH₃I (319 mg, 140 μ L, 2.25 mmol) was added. After the mixture was stirred for 18 h, 50 mL of water was added. The organic layer was separated, and the aqueous solution was extracted with CH₂Cl₂ (2 \times 40 mL). The combined organic phase was dried over anhydrous Na₂SO₄ and evaporated in vacuo, and black solid (192 mg, 0.196 mmol, 93%) was obtained. Crystals suitable for the X-ray analysis were obtained using mixed solvents of hexane and CH₂Cl₂: IR (cm⁻¹, neat) 2953, 2922, 1706, 1489, 1452, 1433, 1365, 1307, 1273, 1231, 1167, 1149, 1135, 1111, 1045, 865, 733, 689; UV–vis (λ_{max} , nm, in CH₂Cl₂) 268 ($\epsilon = 44.8 \text{ mM}^{-1} \text{ cm}^{-1}$), 410 ($\epsilon = 16.2 \text{ mM}^{-1} \text{ cm}^{-1}$), 490 ($\epsilon = 19.6 \text{ mM}^{-1} \text{ cm}^{-1}$); MS (ESI, [M + Na]⁺, *m/z*) 1063.9762 (measured), 1063.9766 (calcd).

Tris(8-acetoxymethoxycarbonyl-2,2,6,6-tetramethylbenzo[1,2-*d*;4,5-*d'*]bis[1,3]dithiol-4-yl)methyl (AMT-03) and Bis(8-acetoxymethoxycarbonyl-2,2,6,6-tetramethylbenzo [1,2-*d*;4,5-*d'*]bis[1,3]dithiol-4-yl)mono(8-carboxyl-2,2,6,6-tetramethylbenzo[1,2-*d*;4,5-*d'*]bis[1,3]dithiol-4-yl)methyl (AMT-02). To a solution of CAT-03 (0.2 g, 0.2 mmol) in 10 mL of DMSO was added solid K₂CO₃ (195.8 mg, 1.42 mmol). The reaction mixture was stirred for 0.5 h, then bromomethyl acetate (107.9 mg, 69.2 μ L, 0.71 mmol) was added. The reaction was stirred for 18 h at room temperature. Water (50 mL) was then added, and the organic layer was separated. The aqueous solution was extracted with CH₂Cl₂ (2 \times 40 mL). The combined organic solution was dried over anhydrous Na₂SO₄ and evaporated in vacuo. The resulting residue was separated and then purified by column chromatography using silica gel and CHCl₃ followed by 10%–90% methanol–CHCl₃ as eluents. The brown solids AMT-03 (93 mg, 0.077 mmol, 39%) and AMT-02 (76 mg, 0.066 mmol, 31.4%) were obtained. AMT-03: IR (cm⁻¹, neat) 2968, 2923, 1769, 1714, 1488, 1452, 1366, 1270, 1226, 1198, 1150, 1127, 1109, 1019, 970, 787, 734, 697; UV (λ_{max} , nm, CH₂Cl₂) 270 ($\epsilon = 46.9 \text{ mM}^{-1} \text{ cm}^{-1}$), 419 ($\epsilon = 19.2 \text{ mM}^{-1} \text{ cm}^{-1}$), 498 ($\epsilon = 21.7 \text{ mM}^{-1} \text{ cm}^{-1}$); MS (ESI, [M + Na]⁺, *m/z*) 1237.9924 (measured), 1237.9927 (calcd). AMT-02: IR (cm⁻¹, neat) 3500 (broad), 2965, 2922, 1769, 1713, 1688 (overlapped with 1713), 1489, 1453, 1366, 1271, 1229, 1200, 1150, 1110, 1020, 972, 787, 725, 696; UV (λ_{max} , nm, CH₂Cl₂) 269 ($\epsilon = 38.3 \text{ mM}^{-1} \text{ cm}^{-1}$), 415 ($\epsilon = 15.3 \text{ mM}^{-1} \text{ cm}^{-1}$), 496 ($\epsilon = 16.9 \text{ mM}^{-1} \text{ cm}^{-1}$); MS (ESI, [M + Na]⁺, *m/z*): 1165.9705 (measured), 1165.9716 (calcd).

EPR Spectroscopy. EPR spectra were recorded at room temperature using X-band spectrometer with high sensitivity resonator. The following acquisition parameters were used in the data acquisition: modulation frequency, 100 kHz; microwave frequency, 9.79 GHz; modulation amplitude, 0.01–0.5; time constant, 41–164 ms; scan time, 42–84 s; and microwave power, 2 mW.

Oxygen Sensitivity. A solution of trityl radical (10 μ M) in DMSO was transferred into a gas-permeable Teflon tube (i.d. = 0.8 mm) and was sealed at both ends. The sealed sample was placed

inside a quartz EPR tube with open ends. Nitrogen or N₂/O₂ gas mixture with varying concentrations of O₂ was allowed to bleed into the EPR tube. After 20 min of equilibration, the EPR spectrum was recorded and the peak–peak line width was calculated.

Cyclic Voltammetry. Cyclic voltammetry was performed on a potentiostat and computer-controlled electroanalytical system. Electrochemical measurements were carried out in a 10 mL cell equipped with a gold working electrode, a platinum-wire auxiliary electrode, and a Ag/AgCl reference electrode. Solutions were degassed by bubbling with the nitrogen gas before the detection. The redox potentials of the ester trityls were referenced internally by using ferrocene. Scan rate (ν) was varied and showed a constant value for $E_{1/2}$. The redox potentials were calculated according to the relation $E = (E_p^a + E_p^c)/2$.

Hydrolysis of Ester-Derivatized Trityls. The in vitro enzymatic hydrolysis of the ester-derivatized trityl radicals was carried out using esterase from porcine liver. Each trityl radical was dissolved in DMSO (5%) to give a final concentration of 10 μ M in phosphate buffer (pH 7.4). PLE (50 U/mL) was added, and the resulting solution was incubated at 37 °C. Sample was taken for EPR or UV–vis spectroscopic analyses at various incubation times (0, 15, 30, 45, and 60 min). Alkaline hydrolysis of the ester-derivatized trityl radicals (10 μ M) was carried out using 25 mM KOH at room temperature.

Computational Methods. Density functional theory (DFT)^{21,22} was applied in this study to determine the optimized geometry and vibrational frequencies at the B3LYP/6-31G* level.²⁷ All calculations were performed using Gaussian 03²⁸ at the Ohio Supercomputer Center. Spin densities were determined for CPh₃ and MT-03

using natural population analyses (NPA)²⁹ at the B3LYP/6-31G* level. Spin contamination for all of the stationary point of the radical structures was negligible, i.e., $\langle S^2 \rangle = 0.75$.

Acknowledgment. This work was supported by National Institutes of Health Grant Nos. EB0890, EB4900 and EB 03519. F.A.V. acknowledges grant support from HL81248. We acknowledge Dr. Christopher M. Hadad for helpful suggestions. The Ohio supercomputer Center is acknowledged in part for support of this work by an allocation of computing time.

Supporting Information Available: X-ray crystallographic details of compound MT-03, cyclic voltammograms, MS spectra, and IR spectra. This material is available free of charge via the Internet at <http://pubs.acs.org>.

JO7022747

(28) Frisch, M. J.; Trucks, G. W.; Schlegel, H. B.; Scuseria, G. E.; Robb, M. A.; Cheeseman, J. R.; Montgomery, J. A., Jr.; Vreven, T.; Kudin, K. N.; Burant, J. C.; Millam, J. M.; Iyengar, S. S.; Tomasi, J.; Barone, V.; Mennucci, B.; Cossi, M.; Scalmani, G.; Rega, N.; Petersson, G. A.; Nakatsuji, H.; Hada, M.; Ehara, M.; Toyota, K.; Fukuda, R.; Hasegawa, J.; Ishida, M.; Nakajima, T.; Honda, Y.; Kitao, O.; Nakai, H.; Klene, M.; Li, X.; Knox, J. E.; Hratchian, H. P.; Cross, J. B.; Bakken, V.; Adamo, C.; Jaramillo, J.; Gomperts, R.; Stratmann, R. E.; Yazyev, O.; Austin, A. J.; Cammi, R.; Pomelli, C.; Ochterski, J. W.; Ayala, P. Y.; Morokuma, K.; Voth, G. A.; Salvador, P.; Dannenberg, J. J.; Zakrzewski, V. G.; Dapprich, S.; Daniels, A. D.; Strain, M. C.; Farkas, O.; Malick, D. K.; Rabuck, A. D.; Raghavachari, K.; Foresman, J. B.; Ortiz, J. V.; Cui, Q.; Baboul, A. G.; Clifford, S.; Cioslowski, J.; Stefanov, B. B.; Liu, G.; Liashenko, A.; Piskorz, P.; Komaromi, I.; Martin, R. L.; Fox, D. J.; Keith, T.; Al-Laham, M. A.; Peng, C. Y.; Nanayakkara, A.; Challacombe, M.; Gill, P. M. W.; Johnson, B.; Chen, W.; Wong, M. W.; Gonzalez, C.; Pople, J. A. *Gaussian 03*, Gaussian, Inc., Pittsburgh PA, 2003.

(29) Reed, A. E.; Curtiss, L. A.; Weinhold, F. A. *Chem. Rev.* **1988**, *88*, 899.

(27) Scott, A. P.; Radom, L. *J. Phys. Chem.* **1996**, *100*, 16502.